Title	Passive RFID at millimeter waves
Author(s)	Pursula, Pekka; Donzelli, Francesco; Seppä, Heikki
Citation	IEEE Transactions on Microwave Theory and Techniques vol. 59(2011):8, pp. 2151-2157
Date	2011
URL	http://dx.doi.org/10.1109/TMTT.2011.2141147
Rights	Copyright © (2011) IEEE. Reprinted from IEEE Transactions on Microwave Theory and Techniques. This article may be downloaded for personal use only

Passive RFID at Millimeter Waves

Pekka Pursula, *Member, IEEE*, Francesco Donzelli, and Heikki Seppä

***Abstract*—This paper introduces a novel way to implement passive RF identification (RFID) at millimeter waves. Passive operation is achieved by adding an external mixing element between the tag antenna and a standard RFID chip. The mixing element converts the RFID reader signal from millimeter waves to RFID carrier frequency—the RFID chip operates as usual. Either passive or semipassive RFID circuits at any RFID carrier frequency can be used. The reader's TX and RX ports are similarly equipped with external mixers to convert the reader output to millimeter waves and received millimeter-wave signal to RFID carrier frequency. The paper analyses the concept theoretically with a Schottky diode as the mixing element. The design and experimental demonstration of the operation at 10 GHz are presented. Using an EPC-compliant UHF tag integrated circuit and reader, a range of 30 cm is demonstrated, but range extension to over a meter is feasible.**

***Index Terms*—Millimeter-wave identification (MMID), RF identification (RFID).**

I. Introduction

RF identification (RFID) has gained a lot of attention recently. Passive RFID technology at UHF has enabled several applications, e.g., tracking of goods in supply chain and asset management. The success of the technology is based on robust identification up to a range of 10 m with inexpensive (even less than 10 Euro cent) tags, and standards [1], [2] that guarantee the interoperability of tags and readers of different manufacturers. However, the readers are bulky due to the big antennas at UHF.

Millimeter-wave RFID (MMID) enables directional reader and tag antennas with practical dimensions [3], [4]. A narrow-beamed highly directional reader antenna enables localization by manual scanning or by angle-of-arrival (AoA). For ranging, similar techniques than at UHF RFID can be used, such as received signal strength (RSSI, e.g., [5]) or phase (e.g., [6]–[8]). Other advantages of MMID include wider available bandwidth, which enables high data-rate short-range communications. The drawback is that the antenna effective aperture is directly proportional to the square of the wavelength, effectively diminishing the available power in the passive tag.

Manuscript received December 22, 2010; revised February 16, 2011 and March 23, 2011; accepted March 26, 2011. Date of publication May 12, 2011; date of current version August 17, 2011. This work was supported in part by the EU Commission under Contract FP7-ICT-2007-1-216049 of the ADOSE Project.

P. Pursula and H. Seppä are with the VTT Technical Research Centre Finland, FI-02044 Espoo, Finland (e-mail pekka.pursula@vtt.fi).

F. Donzelli is with the Dipartimento di Elettronica, Informatica e Sistemistica (DEIS), University of Bologna, 40126 Bologna, Italy (e-mail Francesco.donzelli@unibo.it).

Color versions of one or more of the figures in this paper are available online at http://ieeexplore.ieee.org.

Digital Object Identifier 10.1109/TMTT.2011.2141147

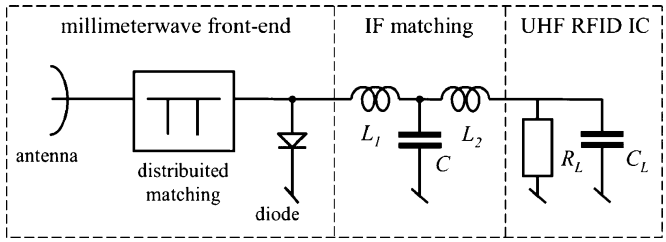

Fig. 1. Block diagram of the proposed millimeter-wave RFID tag.

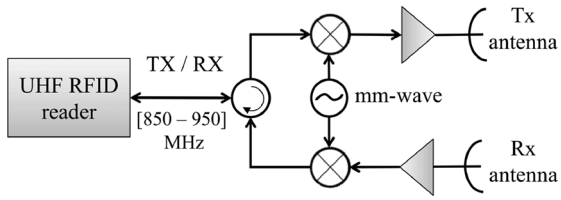

Fig. 2. Reader block diagram.

The key component in the passive tag operation is the rectifier in the tag. Rectification at low power levels is inefficient. At UHF, rectifier efficiencies of 60% are reported [9]. Scaling of CMOS to higher frequencies has also enabled integrated rectifiers at millimeter waves. In [10], an integrated millimeter-wave RFID tag at 60 GHz is reported with rectifier efficiency of 1.2%. The sensitivity of the tag is 2 dBm at a data bandwidth of 5 kbit/s.

In this paper, we present an alternative solution for using millimeter waves for passive RFID. We propose using an external nonlinear component between the tag antenna and UHF RFID IC for mixing millimeter waves to IF frequency suitable for a standard RFID chip, as illustrated in Fig. 1.

The tag receives a millimeter-wave carrier at ω_0 with the UHF RFID signal in sidebands at $\omega_0 \pm \omega_{\mathrm{IF}}$, where ω_{IF} is a frequency in the UHF RFID range (850–950 MHz). The received signal is down-converted in the external mixing element (here a diode) to ω_{IF}. This UHF signal is then fed to the UHF RFID chip, which operates as usual. Modulation of the RFID chip at $\omega_{\mathrm{IF}} \pm \omega_{\mathrm{mod}}$ propagates similarly through the mixing element to frequencies $\omega_0 \pm \omega_{\mathrm{IF}} \pm \omega_{\mathrm{mod}}$, which are then transferred through the tag antenna to the reader.

The reader consists of a standard UHF RFID reader, whose TX/RX output is connected to a circulator (Fig. 2). The TX signals are up-converted in an external mixer to millimeter waves, amplified, and fed to a millimeter-wave antenna. The transmission includes the millimeter carrier frequency ω_0 and sidebands at $\omega_0 \pm \omega_{\mathrm{IF}}$. The received signal is similarly down-converted by an external mixer to $\omega_{\mathrm{IF}} \pm \omega_{\mathrm{mod}}$, which is fed to the standard UHF RFID reader.

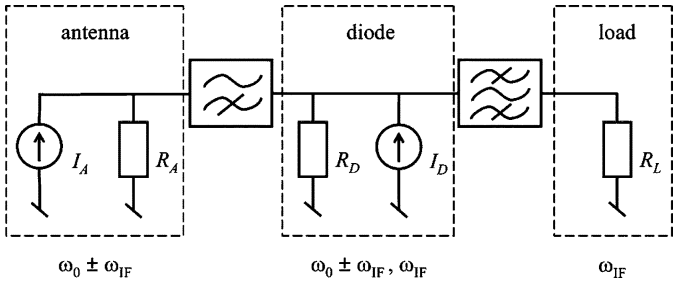

Fig. 3. Circuit schematic for theoretical analysis.

The system enables passive RFID at millimeter waves with standard EPC protocol, including all the features of the UHF RFID, such as anticollision and data rates up to 640 kbit/s. In this paper, operation is demonstrated at 10 GHz, but the idea works at any carrier frequency substantially higher than the frequency of the RFID chip. HF RFID chips could also be used, but their power consumption is higher than UHF chips, leading to an even shorter range. On the other hand, semipassive UHF RFID chips have better sensitivity than passive ones, which would enable higher range.

In this paper, we use a Schottky diode as the mixing element at the tag. Capacitive mixer components, such as varactor diodes, ferroelectric varactors, or microelectromechanical systems (MEMS) resonators could diminish the conversion gain, but no suitable commercial components exist at millimeter waves [11].

This paper is organized as follows. Section II analyses the operation principle of the tag theoretically. Detailed simulation and design of the demonstrator tag at 10 GHz, including the range estimation, is presented in Section III, and experimental verification is presented in Section IV.

II. Theory

Theoretical analysis of the tag can be divided into two separate parts by assuming that the millimeter-wave matching circuit presents a high impedance at UHF, and vice versa. We model the diode as an ideal nonlinear resistor with

$$I_D = I_0\left(e^{qV_D/nkT} - 1\right). \tag{1}$$

Further, we assume constant diode capacitance, which, hence, can be bundled within the matching networks in the following analysis. Omitting the reactive matching, which is assumed ideal, the tag can be presented by the model in Fig. 3. This simple model is enough to illustrate the operation principle of the external mixing element. In practice, the nonlinear capacitance also affects the results, and it is taken into account in the detailed simulation in Section II-A.

A. Power Conversion Efficiency in Forward Link

The antenna is modeled as a current source I_A with internal resistance R_A. The antenna receives three tones from the reader device: carrier at ω_0 and sidebands at $\omega_0 \pm \omega_{\mathrm{IF}}$. The high-pass and bandpass filters divide the circuit in two sub-circuits: The millimeter-wave domain with an antenna and a high-pass filter (HPF), and the diode and the IF domain with the diode and load. The voltage over the diode at perfect match has three components

$$V_D = \frac{R_D}{2}\left\{A_0\sin(\omega_0 t) + \sum_{n=-1,+1} A_n \sin[(\omega_0 + n\omega_{\mathrm{IF}})t]\right\}. \tag{2}$$

The system can be designed for single- or dual-sideband transmission. The former requires only half the bandwidth, but reduces power available for the IF load. The analysis will take this into account by a sideband-signal ratio $s = A_{-1}/A_{+1}$. In practice, the antenna and high-pass filters are optimized for minimum loss at carrier frequency at ω_0 and upper sideband at $\omega_0 \pm \omega_{\mathrm{IF}}$. Hence, the realized sideband constant is somewhere in between the 0 and 1, even though dual-band transmission in the reader is used.

We assume zero dc bias, and use the small-signal model to calculate the diode current I_D at ω_{IF}

$$I_D = \frac{1}{2^2} R_D \gamma A_0 A_{+1}(1+s)\cos(\omega_{\mathrm{IF}} t). \tag{3}$$

Here we have used the relations

$$R_D = \left(\frac{\partial I_D}{\partial V_D}\right)^{-1} \quad \gamma = \left(\frac{\partial^2 I_D}{\partial V_D^2}\right) \Big/ \left(\frac{\partial I_D}{\partial V_D}\right). \tag{4}$$

At perfect match, the power delivered to load R_L is

$$P_L = \frac{A_0^2 A_+^2}{2^7} R_D^3 \gamma^2 (1+s)^2. \tag{5}$$

The power P_A available from the reader field can be similarly calculated

$$P_A = \frac{A_0^2 R_D}{2^3} + \frac{A_+^2 R_D}{2^3}(1+s^2). \tag{6}$$

Forward link conversion efficiency α_f is the ratio of P_L to P_A. The conversion efficiency is directly proportional to the input power, which is easily seen if $A_0 = A_+$ and $s = 0$, giving

$$\alpha_f = \frac{A_0^2}{2^5} R_D^2 \gamma^2 = \frac{P_A}{2^3} R_D \gamma^2. \tag{7}$$

B. Return Link

Communication in the return link is based on backscattering modulation. The UHF RFID chip modulates its input impedance, in this model, its resistance by a value of ΔR_L. The modulation in the chip resistance is seen as a change in the voltage over the diode

$$\begin{aligned} V_D &= \Delta R_L \left(\frac{\partial}{\partial R_L}\frac{R_D R_L}{R_D + R_L}\right) I_D \\ &= \frac{1}{2^4} R_D^2 \gamma \frac{\Delta R_L}{R_L} A_1 A_2 \cos(\omega_{\mathrm{IF}} t) \end{aligned} \tag{8}$$

where the latter equality follows from evaluating the derivative at the complex conjugate match. This voltage represents a third input voltage for the diode, leading to new output current components from the diode nonlinearity. Using similar analysis as

for the forward link, we get the output current component at $\omega_0 \pm \omega_{\rm IF}$

$$I_D = \frac{1}{2^5} R_D^2 \gamma^2 \frac{\Delta R_L}{R_L} A_0^2 \sum_{n=-1,+1} A_n \cos[(\omega_0 + n\omega_{\rm IF})t]. \quad (9)$$

This gives the power delivered to the antenna

$$P_{A,\rm return} = \frac{A_1^4 A_2^2}{2^{13}} R_D^5 \gamma^4 \left(\frac{\Delta R_L}{R_L}\right)^2 (1+s^2). \quad (10)$$

The return link power conversion efficiency α_r is the ratio of the power returned to the antenna $P_{A,\rm return}$ and the power P_A available from the reader field. Evaluating at $A_1 = A_2$ and $s = 0$, we see the quadrature dependence on the input power. The diode attenuates the incoming and outgoing signals equally, as does the free space between the reader and tag

$$\alpha_r = \frac{P_A^2}{2^7} R_D^2 \gamma^4 \left(\frac{\Delta R_L}{R_L}\right)^2 = \frac{1}{2}\left(\frac{\Delta R_L}{R_L}\right)^2 \alpha_f^2. \quad (11)$$

III. Simulations

A. Antenna Design

The necessity to operate at microwave frequencies force us to operate as follows: at the transmitter side, a baseband AM-modulated signal will be produced by an ordinary digital signal processor (DSP)-based RFID reader and internally up-converted to $\omega_{\rm IF}$ in a range of 850–950 MHz. An external customized mixer will then perform the follow-up conversion to $\omega_0 \pm \omega_{\rm IF}$ by a suitable oscillator tone ω_0—in this case, at 10 GHz—at the end of our reading block scheme.

The double up-conversion architecture implies a relative transmitted signal bandwidth of $\omega_{\rm IF}/\omega_0 = 10\%$ at least—by means of a suitable image-rejection mixer—and the necessity to count on wide-bandwidth antennas. An endfire traveling-wave Vivaldi planar topology was preferred due to its simple structure, high gain, good efficiency, and wide bandwidth. Its working mechanism consists of a slotline flared outward to an aperture where the wave impedance matches free space [12]. The most critical elements for the antenna performances, such as microstrip-to-slotline transition and exponential tapered parts, have been analyzed and refined by full-wave electromagnetic (EM) simulation [13] through the finite-element method. Rogers RO4350B ($h = 0.762$ mm, Cu $1/2$ oz, $\varepsilon_r = 3.66, \tan\delta = 0.004$) was chosen for the substrate material. The layout of the antenna is shown in Fig. 4. The differences between measured and simulated return losses (Fig. 5) are most probably due to fabrication tolerance in the very narrow tapered slot in the microstrip-to-slotline transition. The realized antenna does not provide as much selectivity between the sidebands as designed for. Hence, the sideband power ratio s is, in practice, closer to 1 than 0.

The radiation pattern of the antenna is presented in Fig. 6. The single antenna will not provide a narrow enough beam for efficient AoA localization of the tags, and an antenna array would be quite large at 10 GHz. To demonstrate the localization, a higher carrier frequency is required.

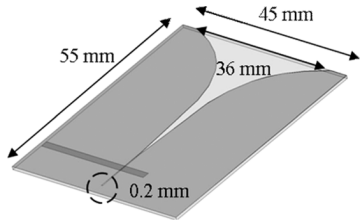

Fig. 4. Vivaldi antenna layout.

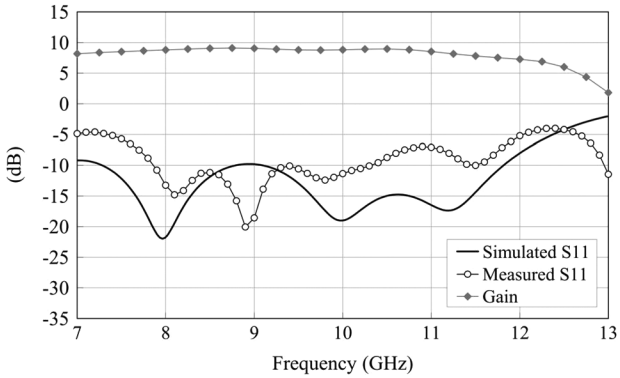

Fig. 5. Antenna return loss and gain.

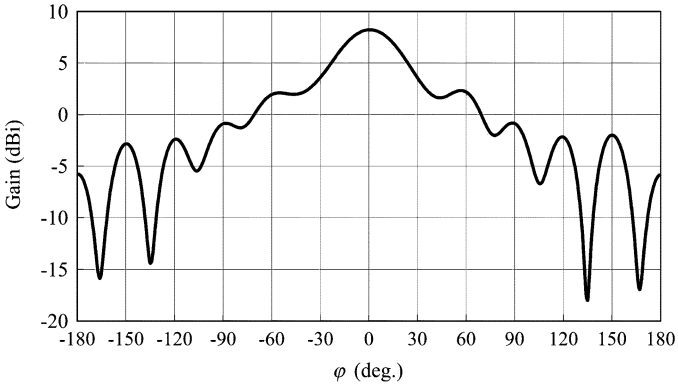

Fig. 6. Simulated antenna E-plane radiation pattern at 10 GHz.

B. Front-End Design Considerations

Since the ordinary RFID chip is expected to be operating at UHF (850–950 MHz), the tag working principle will basically consist of a nonlinear harmonic generation provided by a single-diode mixer—simplest and most effective topology in the present case—with local oscillator tuning furnished by the incoming continuous wave at ω_0 from the transmitter: the load will be only interested by the intermodulation product at $\omega_{\rm IF}$ at the chip's side. A key feature in the mixer design is the choice for a suitable diode, in this case, an Avago Technologies HSMS-286B ($C_{J0} = 0.18$ pF, $I_S = 50$ nA, $N = 1.08$, and $V_J = 0.65$ V). The matching section between antenna and nonlinear device was designed using a conversion gain optimization goal in EM simulation software [14]. The simulations fully take into account the nonlinear capacitance of the diode.

Inside the optimization loop, without any loss of generality, we will assume that the two driving signals are sinusoidal with

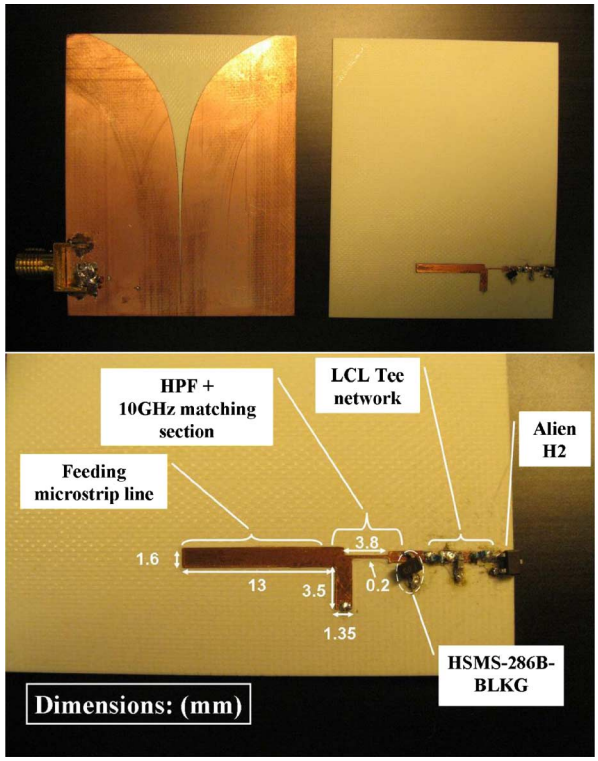

Fig. 7. Final tag detailed view.

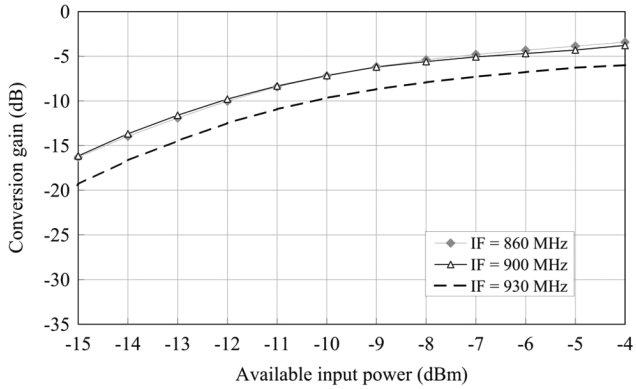

Fig. 8. Simulated conversion gain as a function of input power and IF frequency.

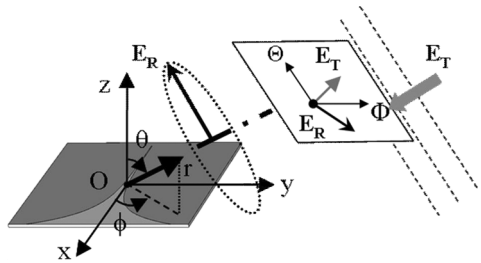

Fig. 9. Tag in presence of an IPW.

incommensurate fundamental frequencies ω_0 and $\omega_{\rm IF}$. A minimum power of -14 dBm at $\omega_{\rm IF}$ is required for the selected RFID IC—Alien Technologies Higgs 2—in the acknowledgement phase. A block diagram of the tag is presented in Fig. 1 and a photograph of the tag is presented in Fig. 7.

The whole front-end can be roughly divided into two distinct subnetworks according to the respective working frequencies: the first one, depicted as the RF network, provides for a conjugate matching between the antenna and the front-end in the neighborhood of the carrier wave—thus considering $\omega_{\rm IF}$ as generically comprised in a range of 850–950 MHz depending on the communication protocol standard; at the same time, an HPF at 9.1 GHz is inserted to operate in conjunction with the antenna return loss for reflecting the consistent near-carrier intermodulation products back to the IF network. The HPF is simply realized by a shunt short stub followed by a microstrip line.

The lumped Tee section is introduced as a bandstop filter for a 10-GHz harmonic, exploiting the inductors' self resonances—in this case, 12 and 5.5 GHz, respectively. Final values for the three lumped elements are $L_1 = 3.3$ nH, $L_2 = 4.3$ nH, and $C = 1.5$ pF, respectively.

To the authors' experience, a lumped shunt *RC* equivalent circuit is sufficient to model the electrical chip behavior: in this case, the nominal values of $R_L = 1500\ \Omega$ and $C_L = 1.2$ pF were assigned and then successfully checked. All the blocks have been modeled with the package parasitic capacitances and inductances. The simulated conversion gain of the entire passive front-end is given in Fig. 8.

C. Range Estimation

An accurate evaluation of the power available to the integrated circuit (IC) is developed by combining the reciprocity theorem with the antenna performances, computed by EM simulation [15]. Such an approach was demonstrated to be able to avoid some ineffectiveness of the Friis equation when the far-field assumption in the link analysis between Reader and Tag is disregarded (e.g., dist$<10\lambda$ with λ as the free-space wavelength at the frequency of interest). Furthermore, port mismatch and power transfer effects between the antenna elements and the nonlinear subsystems are now rigorously accounted for [16]. Here we follow the classic EM formalism (Fig. 9) to specify a field source in terms of known current source and refer to the Norton-equivalent representation for the tag circuit (Fig. 2).

The current source $I_A(\omega)$—depending only on the electric field $\mathbf{E_T}$ of the incoming plane wave (IPW) from the transmitter—plays the role of free source in the receiver analysis and can be computed in two steps: first the incident field is temporarily suppressed and the receiving antenna is employed in a transmitting mode. Through an arbitrary excitation by a current density I injected at the input port, the antenna can be analyzed by a commercial 3-D EM simulator [13] in order to derive both the radiated far-field distribution and the frequency-dependent antenna admittance $Y_A(\omega) = [R_A(\omega)]^{-1}$ at all the frequencies of interest. If we denote the former by $\mathbf{E_R}(r_A, \theta_A, \phi_A; \omega)$ in a suitable receiver-referred spherical reference frame, the result from EM analysis would generally be the complete set of the scalar components of the normalized field $\mathbf{E_{Rn}}(\theta_A, \phi_A; \omega)$

$$\mathbf{E_{Rn}}(\theta_A, \phi_A; \omega) = r_A \cdot \exp(j\beta r_A) \frac{\mathbf{E_R}(r_A, \theta_A, \phi_A; \omega)}{I} \tag{12}$$

where r_A is the generic distance at which $\mathbf{E_R}$ is evaluated.

As a second step, the antenna is used in a receiving mode in the presence of $\mathbf{E_T}$ so that by (13) coincides with the port current. A straightforward application of the reciprocity theorem leads to the following form generated by the relationship between the fields and associated currents:

$$I_A(\omega) = j\frac{2}{\eta}\lambda Y_A(\omega) \cdot \mathbf{E_{Rn}}(\theta_A, \phi_A; \omega) \bullet \mathbf{E_T}(r, \theta_I, \phi_I; \omega) \tag{13}$$

where r is the read range, (θ_I, φ_I) is the angular coordinates of the direction of incidence of $\mathbf{E_T}$ in its respective reference frame (usually different from the receiver-referred one), and η is the free-space impedance. It is noteworthy to mention that the source I_A is independent of the excitation I and is only a function of the IPW field and direction of incidence.

By means of such an approach, a first evaluation of the effective read range can be performed by starting from some average values of equivalent radiated power (ERP) from the transmitter: with 23 dBm ERP, the required -14-dBm power level to the Alien chip can be guaranteed at about 15-cm distance. At the same distance, by making use of (11), the backscattered signal power is proven to fulfill a standard reader sensitivity of roughly -80 dBm—a huge noise contribution among the entire block chain should be considered. Here the atmospheric attenuation (15 dB/km at 60 GHz) can be neglected because the distances are small. For 1-m radio path length, the additional attenuation due to atmosphere is 0.015 dB.

Of course the read range might be considerably increased through a suitable active device at the reader side such as a high-gain power amplifier. Using a more directive reader antenna would increase the TX power to 30-dBm ERP, a power level comparable to a standard UHF RFID reader output. This would extend the range to 30 cm. Adding a higher gain tag antenna would also extend the range: e.g., a $2 * 2$ patch antenna provides fourfold gain, or twofold range compared to a single patch or a Vivaldi. The array is similar to UHF RFID tag antennas in size ($5 * 5$ cm^2). Further, using a semipassive tag IC, the tag sensitivity could be reduced at least to -26 dBm. Since the conversion gain also scales with the incoming power, this would only give twofold range extension. Hence, the range can be extended to over a meter. Capacitive mixing might help to extend the range further, especially with the extremely low input power of semipassive UHF RFID tags.

IV. Measurements

A. Forward Link Performance

The forward link conversion gain was measured by means of a continuous wave feeding system: a block scheme is given in Fig. 10 with the authentic tag load replaced by the 50-Ω spectrum analyzer input impedance. For the measurement, a new matching network at IF was implemented ($L_1 = 3.3$ nH, $L_2 = 22$ nH, $C = 4.6$ pF) to match the 50-Ω load to the diode. This loads the diode with $R_L = 4.8\,\Omega$.

In the measurements, the power of the carrier at ω_0 and the upper sideband $\omega_0 + \omega_{\mathrm{IF}}$ were tuned to -10 dBm at the diode input. The lower sideband power at $\omega_0 - \omega_{\mathrm{IF}}$ was allowed to vary a few decibels in order to keep the carrier and upper sideband

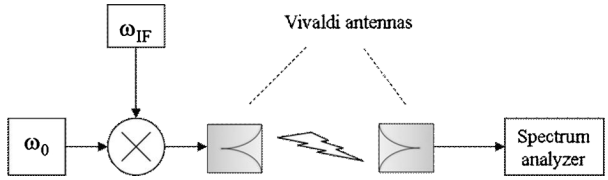

Fig. 10. Forward link measurement setup.

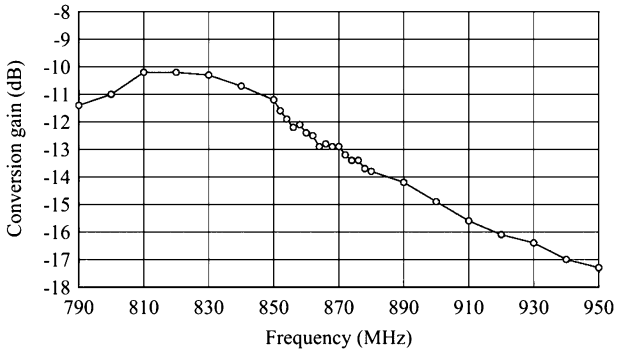

Fig. 11. Measured conversion gain of the diode at -10-dBm input power at carrier and upper sideband as a function of the IF frequency.

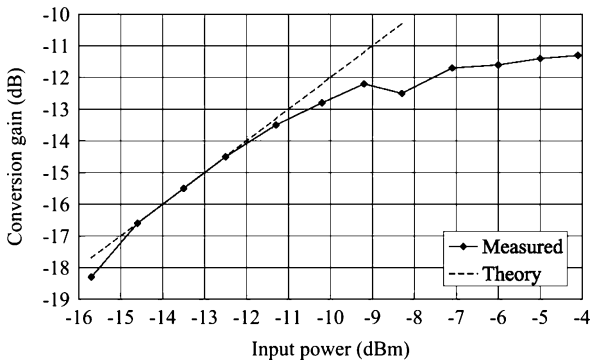

Fig. 12. Measured conversion gain of the front end at 860-MHz IF frequency as a function of the input power at carrier and upper sideband.

powers constant. The measured conversion gain is presented in Fig. 11 as a function of IF frequency. The IF matching is at its best at 820 MHz, where a conversion gain of about -10 dB is achieved. The conversion gain at the nominal operation frequency of 860 MHz is 2.2 dB lower.

Power sweep measurement in Fig. 11 was carried out at the nominal operation frequency of 860 MHz. The theoretical curve is calculated using (10) and subtracting the measured mismatch of 2.2 dB seen in Fig. 12. The measured conversion gain is in agreement with the theory at low input power. Hence, the capacitive mixing in the diode seems not to be of high importance in the demonstrator system. Of course, the small-signal model of Section II cannot predict the saturation, but the simulations in Fig. 8 and the measurements show a similar saturation behavior. However, the measurements exhibit lower conversion gain, most probably due to the fact that the IF matching is not optimized at 860 MHz—this is also seen in the simulations, where the conversion gain at 930 MHz–70 MHz above the nominal IF matching frequency—shows a flatter power response. The sensitivity of the tag at the optimum frequency is -4 dBm, which

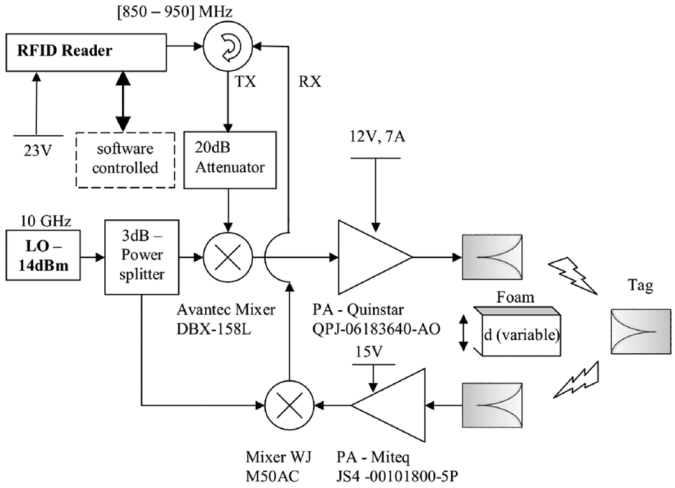

Fig. 13. Read range measurement setup schematic.

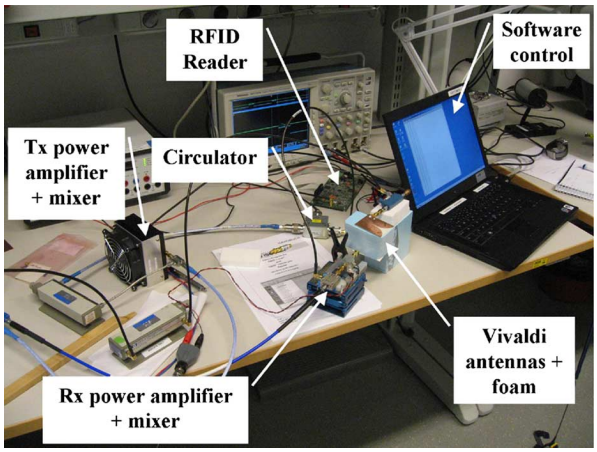

Fig. 14. Read range measurement setup photograph.

is 6 dB better than the passive MMID tag IC in [10]. The power level is feasible for short-range data transfer.

B. Full Operation

Finally, a full system, as depicted in Figs. 13 and 14, was constructed for determining the actual read range: for sake of simplicity, a two-element Vivaldi array is employed as a transceiver at the reading side. Setup enhancements include two high-gain power amplifiers (Quinstar QPJ and Miteq JS4), positioning and tuning of reader RX and TX antenna separation, as well as reader output power control at the RFID reader in order to keep the optimum feeding condition $A_1 = A_2$ (see Section II-A). The transmit power in the measurement is about 30-dBm ERP over the frequency range. FM0 encoding at 40 kbit/s is used for the return link.

The measured tag range was about 30 cm. About 5-cm longer range was observed with the first query of the EPC protocol than with the acknowledgement including the EPC code. The IF frequency sweep in Fig. 15 shows high variation of the read range, which is probably due to two reasons. First, the laboratory demonstrator measurement setup can give rise to standing

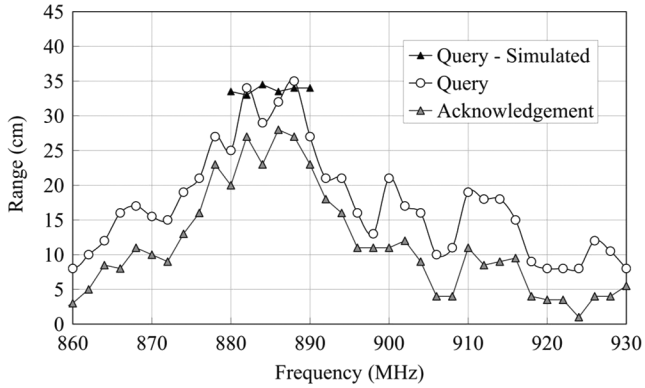

Fig. 15. Measured read range as a function of IF frequency.

waves and multipath propagation effects that are enhanced by the higher carrier frequency. Secondly, the power of the up-converted RFID reader signal was frequency dependent, leading to manual adjustment of the output power of the RFID reader at every frequency point. In addition to this, the achieved suppression of the lower sideband at $\omega_0 - \omega_{\mathrm{IF}}$ in the antenna and matching network was lower than expected. Hence, the lower sideband propagates somewhat to the diode, contributing to the mixing results. Taking into account these nonidealities in the measurement setup, the measured results are in line with the simulated range.

V. Conclusion

This paper has introduced a novel way to implement passive RFID at millimeter waves. The passive operation is achieved by adding an external mixing element between the tag antenna and a standard RFID chip. The mixing element converts the RFID reader signal from millimeter waves to RFID carrier frequency. The reader's TX and RX ports are similarly equipped with external mixers to convert the reader UHF output to millimeter waves and received signal millimeter-wave signal to RFID carrier frequency.

The paper has demonstrated the operation principle at 10 GHz with an EPC-compliant UHF tag IC. A Schottky diode was used as the mixing element. The diode achieved a measured conversion gain of -10 dB from millimeter waves to UHF at the operation power level of the tag. The measured sensitivity of the tag is -4 dBm. The tag was read using a standard EPC reader up to 30 cm with a data rate of 40 kbit/s. The operation range can be extended to over a meter by using more sensitive RFID chips, e.g., semipassive chips, and in the future by using a capacitive mixing element, such as a varactor diode or a ferroelectric varactor.

Acknowledgment

The authors wish to thank Prof. Al. Costanzo and Prof. D. Masotti, both with the University of Bologna, Bologna, Italy, for collaboration. The authors also thank Dr. V. Viikari, VTT Technical Research Centre Finland, Espoo, Finland, for fruitful discussion, and I. Marttila, VTT Technical Research Centre Finland, for help during the measurements.

REFERENCES

[1] "EPC radio-frequency identity protocols, class-1 generation-2 UHF RFID, protocol for communications at 860 MHz - 960 MHz, version 1.2.0," EPCglobal, 2008. [Online]. Available: http://www.gs1.org/epcglobal/

[2] *Radio frequency identification for item management: Parameters for air interface communications at 860 MHz to 960 MHz*, ISO/IEC 18000-6, 2010 [Online]. Available: http://www.iso.org

[3] P. Pursula, T. Vähä-Heikkilä, A. Müller, D. Neculoiu, G. Konstantinidis, A. Oja, and J. Tuovinen, "Millimetre wave identification—New radio system for low power, high data rate and short range," *IEEE Trans. Microw. Theory Tech.*, vol. 56, no. 10, pp. 2221–2228, Oct. 2008.

[4] D. Neculoiu, G. Konstantinidis, T. Vähä-Heikkilä, A. Müller, D. Vasilache, A. Stavinidris, L. Bary, M. Dragoman, I. Petrini, C. Buiculescu, Z. Hazoupulos, N. Kornilios, P. Pursula, R. Plana, and D. Dascalu, "GaAs membrane-supported 60 GHz receiver with Yagi–Uda Antenna," in *8th Int. RF MEMS RF Microsyst. Symp.*, Barcelona, Spain, Jun. 2007, pp. 15–18.

[5] J. S. Choi, H. Lee, R. Elmasri, and D. W. Engels, "Localization systems using passive UHF RFID," in *5th Int. NC/IMS/IDC Joint Conf.*, Seoul, Korea, Aug. 2009, pp. 1727–1732.

[6] P. V. Nikitin, R. Martinez, S. Ramamurthy, H. Leland, G. Spiess, and K. V. S. Rao, "Phase based spatial identification of UHF RFID tags," in *IEEE Int. RFID Conf.*, Orlando, FL, Apr. 2010, pp. 102–109.

[7] V. Viikari, P. Pursula, and K. Jaakkola, "Ranging of UHF RFID tag using stepped frequency read-out," *IEEE Sens. J.*, vol. 10, no. 9, pp. 1535–1539, Sep. 2010.

[8] D. Arnitz, K. Witrisal, and U. Muehlmann, "Multifrequency continuous-wave radar approach to ranging in passive UHF RFID," *IEEE Trans. Microw. Theory Tech.*, vol. 57, no. 5, pp. 1398–1405, May 2009.

[9] V. Rizzoli, F. Donzelli, A. Costanzo, and D. Masotti, "Integration of numerical and field-theorical techniques in the design of single- and multi-band rectennas for micro-power generation," *Int. J. Microw. Wireless Technol.*, vol. 2, pp. 293–303, Jul. 2010.

[10] S. Pellerano, J. Alvarado, and Y. Palaskas, "A mm-wave power harvesting RFID tag in 90 nm CMOS," in *Custom Integr. Circuits Conf.*, San Jose, CA, Sep. 2009, pp. 677–680.

[11] V. Viikari, M. Kantanen, T. Varpula, A. Lamminen, A. Alastalo, T. Mattila, H. Seppa, P. Pursula, J. Saebboe, S. Cheng, M. Al-Nuaimi, P. Hallbjorner, and A. Rydberg, "Technical solutions for automotive intermodulation radar for detecting vulnerable road users," in *IEEE 69th Veh. Technol. Conf.*, Barcelona, Spain, Apr. 2009, pp. 1–5.

[12] P. J. Gibson, "The Vivaldi aerial," in *Proc. 9th Eur. Microw. Conf.*, 1979, pp. 101–105.

[13] Ansoft HFSS 3-D Full-Wave Electromagnetic Field Simulation Software. ANSYS, Canonsburg, PA, 2010. [Online]. Available: http://www.ansoft.com/products/hf/hfss/

[14] AWR-MWO Design Environment. AWR, El Segundo, CA, 2010. [Online]. Available: http://web.awrcorp.com/

[15] V. Rizzoli, A. Costanzo, and G. Monti, "General electromagnetic compatibility analysis for nonlinear microwave integrated circuits," in *IEEE MTT-S Int. Microw. Symp. Dig.*, Jun. 2004, pp. 953–956.

[16] V. Rizzoli, F. Donzelli, P. Spadoni, A. Costanzo, D. Masotti, and E. M. Vitucci, "A CAD procedure for MIMO link estimation by the combination of nonlinear, electromagnetic and propagation analysis techniques," in *IEEE MTT-S Int. Microw. Symp. Dig.*, Atlanta, GA, Jun. 2008, pp. 927–930.

Pekka Pursula (M'09) was born in Vantaa, Finland, in 1978. He received the M.Sc. degree (with distinction) and D.Sc. degree in technical physics from the Helsinki University of Technology (TKK), Espoo, Finland, in 2002 and 2009, respectively.

In 2002, he was with Philips Medical Systems Finland, where he developed RF systems in magnetic resonance imaging (MRI). Since 2003, he has been with the VTT Technical Research Centre of Finland, Espoo, Finland, where he is a Senior Research Scientist. He has authored or coauthored over 20 peer-reviewed journal and conference papers. His research interests include RFID systems at UHF and millimeter waves, as well as wireless sensors.

D.Sc. Pursula was the recipient of the Young Scientist Award of the 2004 URSI/IEEE XXIX Finnish Convention on Radio Science.

Francesco Donzelli received the Dr. Ing. degree in telecommunication engineering from the University of Bologna, Bologna, Italy in 2007, and is currently working toward Ph.D. degree in telecommunication engineering at the University of Bologna.

He has coauthored several international papers. His current research interests focus on characterization of RF links by the combination of nonlinear, EM, and propagation analysis techniques, but comprise also the project and realization of low-power rectennas for energy harvesting from wireless sources, and the design and analysis of RF microelectromechanical devices.

Dr. Donzelli was the recipient of the 2010 Dipartimento di Elettronica, Informatica e Sistemistica (DEIS) Best Paper Award from the University of Bologna for his last publication on efficient energy harvesting.

Heikki Seppä was born in Kortesjärvi, Finland, in 1953. He received the D.Sc. (Tech.) degree from the Helsinki University of Technology (TKK), Espoo, Finland, in 1989.

From 1976 to 1979, he was an Assistant with TKK, where he studied low-temperature physics and electrical metrology. In 1979, he joined the Technical Research Centre, Espoo, Finland, where he mainly developed the quantum metrology. In 1989, he became a Research Professor with VTT Technical Research Centre Finland, Espoo, Finland. His research is focused on metrology, quantum devices, sensors, and especially on microelectromechancial systems (MEMS), wireless technology, and nanotechnology. From 1982 to 1983, he spent several months with the National Institute of Standards and Technology (NIST), Boulder, CO, where he developed ultra-low-temperature noise thermometers. In 2004, he was a Tutoring Professor with Nokia's Leading Science Program.